COMPDYN 2011
3rd ECCOMAS Thematic Conference on
Computational Methods in Structural Dynamics and Earthquake Engineering
M. Papadrakakis, M. Fragiadakis, V. Plevris (eds.)
Corfu, Greece, 25–28 May 2011

FRAGILITY CURVES FOR TYPICAL MULTISPAN SIMPLY SUPPORTED BRIDGE CLASSES IN MODERATE SEISMIC ZONES: PRE- AND POST-SEISMIC DESIGN CONSIDERATIONS

Karthik Ramanathan[1], Jamie E. Padgett[2], and Reginald DesRoches[1]

[1] School of Civil and Environmental Engineering, Georgia Institute of Technology
790 Atlantic Drive, Atlanta, GA 30332-0355.
e-mail: karthik.ramanathan@gatech.edu, reginald.desroches@ce.gatech.edu

[2] Department of Civil and Environmental Engineering, Rice University
6100 Main Street, MS-318, Houston, TX 77005.
e-mail: jamie.padgett@rice.edu

Keywords: Fragility curves, analytical modeling, seismic design, non-seismic design, bridge classes, HAZUS-MH comparison.

Abstract. *Multispan simply supported concrete and steel girder bridges are common bridge types in Central and Southeastern United States. Probabilistic seismic risk assessment of these bridge classes is essential due to an increased awareness of the seismic hazard in the region. This study focuses on developing and comparing fragility curves for seismically and non-seismically designed bridges that are common in the region. Detailed three dimensional nonlinear analytical models, which account for the nonlinear behavior of the columns, girders and abutments, are developed in OpenSEES platform. Unlike most previous studies, the fragility curves are developed considering a wide range of material and geometric uncertainties in the stochastic analyses coupled with considerations of vulnerability of multiple components in defining bridge system performance. The results provide insight into the level of uncertainty introduced in the analysis of fragility curves for portfolios of bridges with the use of three dimensional analytical models and nonlinear time history analyses. Component and system fragility curves are obtained and are compared for the case of non-seismically and seismically designed bridge classes and with those currently used in HAZUS-MH.*

1 INTRODUCTION

Fragility curves, which are conditional probability statements that give the likelihood that a structure will meet or exceed a specified level of damage for a given ground motion intensity measure, have found widespread use in probabilistic seismic risk assessment of highway bridges. The conditioning parameter is typically a single intensity measure such as peak ground acceleration (PGA) or spectral acceleration at the geometric mean of the longitudinal and transverse periods ($S_{a\text{-}gm}$). They are a fundamental building block used in multiple (current and potential future) applications including emergency response, design support such as performance based earthquake engineering, planning support involving assessment of traffic impacts and possible economic losses post a seismic event, and policy support.

The earliest attempt to formalize seismic risk assessment procedures is found in the seminal work by Whitman et al. [1]. Since then several attempts have been made to quantify the risk to highway infrastructure systems. The Applied Technology Council took the first step in performing seismic risk assessment [2] of infrastructure for the state of California using damage probability matrices and restoration functions. Since then several committees constituted by ATC have been solely devoted to the risk assessment of lifelines. The ATC 25 report [3] introduced the concept of continuous fragility functions for lifeline systems including bridges by performing regression on the discrete values of damage probability matrices. Further attempts to push forward the seismic risk assessment methods were made by the Federal Emergency Management Agency (FEMA) by the constitution of a committee of experts and introduction of a Geographic Information Systems (GIS) based risk assessment software, Hazards United States [4] in 1997. Since then HAZUS has undergone several improvements and revisions and now includes models for estimating potential losses from a variety of natural disasters like earthquakes, floods and hurricanes.

Over the years, structural fragilities have been determined in a variety of ways. The ATC 13 Report documents risk assessment of the infrastructure stock in California essentially based on expert opinion. A panel of 42 experts was assembled to develop damage probability matrices for bridge infrastructure based on their expertise. This technique has several major concerns since the procedure is totally subjective and depends on the number of experts queried and therefore is based on expertise and experience of the individuals with little correlation to actually observed earthquake damage. The 1989 Loma Prieta, 1994 Northridge and 1995 Kobe earthquakes were watersheds for fragility research. Several researchers [5, 6, 7, 8, 9, 10] developed empirical fragility curves based on actual damage data observed in these earthquakes. Although the adopted procedure differed slightly among the researchers, the general essence was the same. Basoz and Kiremidjian [5] assembled damage frequency matrices and performed a logistic regression analysis to develop fragility curves while Shinozula et al. [9] used the Maximum Likelihood Method to estimate the parameters of a lognormal probability distribution describing the fragility curves. Der Kiureghian [7] employed a Bayesian approach in order to develop fragility curves. However, lack of sufficient damage data, discrepancies in the damage assessments in the aftermath of a seismic event, variation in the ground motion intensities at the damage sites depending on the earthquake source are some of the limitations of this technique for developing fragility curves.

Advances in modeling capabilities coupled with lack of sufficient earthquake damage data drove the development of fragility curves using analytical methods. Yu et al. [11] used simple single-degree-of-freedom models and elastic response spectrum analysis to develop fragility curves for highway bridges in Kentucky while Hwang et al. [12] furthered this approach with slight modifications. Dutta [13] and Basoz and Mander [14] used the Nonlinear Static Procedure commonly referred to as the Capacity Spectrum Method (CSM) to develop fragilities for

highway bridge classes in the United States. Currently these values are employed in HAZUS-MH for seismic risk assessment of highway infrastructure systems. Several researchers resorted to more reliable yet computationally expensive techniques like Nonlinear Time History Analysis (NLTHA) and Incremental Dynamic Analysis (IDA) to develop fragility curves. Mackie and Stojadinovic [15] employed NLTHA and IDA to develop fragility curves. These formed the basis of a rational methodology to evaluate damage potential and to assess probable highway bridge losses for critical decision making regarding post earthquake safety and repairs to highway networks. Nielson et al. [16], Padgett et al. [17], Ramanathan et al. [18] employed NLTHA to develop fragility curves for as-built and retrofitted bridge classes in Central and Southeastern United States (CSUS) accounting for multiple component vulnerability.

This study develops analytical fragility curves for seismically (S-) and non-seismically (NS-) designed multispan simply supported (MSSS) bridge classes in the CSUS to provide new insight on the relative vulnerability of these classes of bridges considering distinct levels of seismic design. The following eleven states are considered in the analysis: Arkansas, Alabama, Georgia, Illinois, Indiana, Kentucky, Missouri, Mississippi, North Carolina, and South Carolina. A detailed review of bridges in the NBI [19] in the CSUS region shows MSSS concrete and steel girder bridge classes account for approximately 20% of the bridges in the region. In 1990, bridges in the CSUS began incorporating seismic details. The bridges in the CSUS built prior to 1990 have several known seismic deficiencies which include non-ductile steel bearings, short seat widths, non-ductile columns, high pounding potential and the increased potential for the toppling of rocker bearings [20]. Some of the changes post-1990 included the component design forces, design of columns and foundation, bearing types, and treatment of liquefaction and liquefaction induced ground movement. A review of the evolution in seismic design practices in the region reveals that the predominant difference between seismically and non-seismically designed bridges is associated with the detailing aspects in the columns and the replacement of the steel rocker bearings with elastomeric bearing pads with steel dowels, as presented in detail in the next section of the paper. Bridge piers designed in the CSUS after 1990 have greater splice lengths and transverse reinforcement ratios in the longitudinal and transverse directions, when compared to the respective values in columns designed prior to 1990. The steel rocker bearings are often replaced with elastomeric bearing pads with steel dowels. Their flexibility allows the superstructure to be decoupled from the substructure yet they may also render susceptibility to large deck displacements as well as the potential for bearing walk out from under the girders.

While previous studies [16, 21, 12] have evaluated the seismic response and fragility of various bridge classes common to the CSUS, there is very little research that explores the differences in performance of typical CSUS bridge classes built with and without seismic detailing. This paper addresses this gap by investigating the influence of seismic detailing of the two multispan bridge classes on the seismic performance, as well as the failure probability through the development and comparison of fragility curves.

2 PRE- AND POST-SEISMIC DESIGN CONSIDERATIONS IN CSUS

This paper assesses the effect of seismic design detailing on typical MSSS concrete and steel girder bridge classes in the CSUS through the development of analytical fragility curves. As previously stated, the predominant difference between the non-seismically (NS-MSSS) and seismically (S-MSSS) designed bridges considered in this study is associated with the enhanced ductility characteristics of the columns in terms of detailing aspects and the replacement of non-ductile steel bearings with elastomeric bearing pads having steel dowels. Bridges constructed prior to 1990 in the CSUS region are typically not designed for the adequate

seismic hazard in the region. Non-seismically designed bridges with steel girders in their superstructure typically use one of the two general classes of steel bearings, viz. high type and low type. Both of these bearing types include a fixed or pinned type bearing and an expansion type bearing with the difference being the type of motion associated with the latter. In the case of high type bearings, the motion associated with the expansion bearing is based on a rocking mechanism while it is characterized by sliding in the case of the low type bearing. In the case of MSSS steel girder bridge class, these bearing types are replaced by elastomeric bearing pads with steel dowels in addition to the reduced transverse reinforcement spacing in the columns. The relative flexible nature of these elastomeric bearings allows the superstructure to be decoupled from the substructure, and hence these bearings are susceptible to large deformations, which will be illustrated in subsequent sections of the paper. However, these large deformations could cause unseating of the bridge girders and may also result in bearings walking out from under the girders. In case of both NS- and S-MSSS concrete girder bridges, the bearings adopted were elastomeric bearing pads with steel dowels.

The reduced spacing of the transverse reinforcement in the columns is the primary difference considered between seismically and non-seismically designed columns in both bridge class columns. It is well known that column transverse reinforcement has a major impact on the shear resistance, and ductility capacity of bridges. Prior to 1990, bridge columns in the CSUS typically had transverse reinforcement which consisted of #13 bars at a spacing of 305 mm on center. Whereas, in case of the seismically designed bridges, the spacing of the #13 stirrups is as close as 76 mm on center thereby making flexure the predominant behavioral mode. In either case, the bridges have multi column bents often consisting of a rectangular reinforced concrete bent beam (Figure 1) supported by 914 mm diameter circular columns. The effect of closely spaced transverse reinforcement is incorporated by an increase in the confined compressive strength of concrete and ductility by specifying higher ultimate strain using the concrete model proposed by Mander et al. [22]. Further details can be found in [18]. In the case of the seismically designed columns, the confined compressive strength, f_{con} is approximately 33% larger than characteristic concrete strength, f'_c and the ultimate strain, ε_{cu} is approximately 0.05. Whereas, in the case of the non-seismically designed bridge columns, f_{con} is approximately 7.1% larger than f'_c and ε_{cu} is only about 0.012. Other column details such as lap splices in plastic hinge regions are not considered explicitly in the current study's column models.

3 SEISMICALLY AND NON-SEISMICALLY DESIGNED BRIDGE CLASS CASE STUDIES

The following sections present detailed information on the bridge class characteristics, analytical modeling procedures and provide some insight on the change in dynamic characteristics with the incorporation of seismic design principles. It moves on with the development of PSDMs and having characterized damage, demonstrates the development of component level fragility curves, which provides a means to look at the relative vulnerability of components in the seismic and non-seismically designed bridges.

3.1 Bridge Class Characteristics

Basic geometric characteristics of the bridge, such as number of spans, span length, deck width, and column height are analyzed and empirical cumulative density functions (CDF) are developed for each of these parameters. Twelve representative bridge configurations are generated using Latin Hypercube sampling from these empirical CDFs for the geometric parameters. The distributions are consistent with those presented in [16] to facilitate comparison.

Based on the inventory analyses, analytical bridge models are created with three spans and zero skew across all bridge classes as these were the most likely bridge configurations. Typical details for these bridge classes can be found in [21, 16], and these are consistent with [12] for Memphis, TN and [23] for Southern IL. The pre- and post-seismic design considerations for the respective bridge classes were discussed in the preceding section.

3.2 Analytical Bridge Models

The typical layout of a three span zero skew bridge is shown in Figure 1. The bridges are modeled in three dimensions using the finite element platform OpenSEES [24] incorporating both geometric and material nonlinearities. The superstructure is modeled using elastic beam-column elements with mass lumped along the centerline. This is typical as the composite slab and girder generally behave linearly. Pounding between the decks is considered using the contact element approach developed by Muthukumar and DesRoches [25]. This approach explicitly accounts for the effects of loss of hysteretic energy. Rayleigh damping is used in the model but is treated as a random variable. Nonlinear beam column elements with fiber defined cross sections are used to model the columns. The nonlinear hysteretic behavior of these columns is captured using a distributed plasticity element. Fiber defined cross sections enable specifying different properties for cover concrete and confined concrete. The differences in the modeling of the seismically and non-seismically designed columns are incorporated using the concrete model. The effect of the closely spaced transverse reinforcement in the case of the seismically designed bridge columns is accounted for by using the confined concrete model discussed in the previous section.

The bearings, both steel and elastomeric bearing pads with steel dowels, are modeled using nonlinear translational springs. In case of the elastomeric bearings, this accounts for the contribution of the elastomeric pads in addition to the steel dowels in the bearing elements. The behavior of steel bearings in both longitudinal and transverse directions is modeled according to the recommendations of Mander et al. [26] stemming from an experimental study. Abutments provide both longitudinal and transverse restraint to the bridge superstructure under loading in both directions. The longitudinal resistance is comprised of both passive and active components. The former is partially provided by soil and by the piles while the latter is provided only by the piles. This study adopts the recommendations of Caltrans [27] in estimating the stiffness of the abutments which are modeled using nonlinear translational springs. Further, the Caltrans recommendations [27] suggests that the effect of wing-walls decreases as the width of the abutment increases and therefore the transverse resistance is conservatively assumed to be provided solely by the piles. The foundation system of most of the highway bridges in CSUS consists of piles [12] which are modeled using nonlinear translational and rotational springs. The stiffness used here is the average stiffness by considering both rigid and flexible nature of the piles. The composite behavior is then computed following some basic geometry based equations presented in [28].

3.3 Deterministic Bridge Responses

In order to understand the effect of seismic detailing principles on the dynamic characteristics of the bridge, one sample set of responses from the NLTHA is compared prior to presenting the PSDMs. In this sample, identical geometries of seismically and non-seismically designed bridges with all the variables set to their median values are subjected to the same ground motion with geometric mean of the PGA of two orthogonal components equal to $0.62g$. Therefore, the only distinction rests with the incorporation of seismic provisions viz.,

enhanced ductility in the columns in all bridge classes and replacement of steel bearings with elastomeric bearing pads in the steel bridge classes.

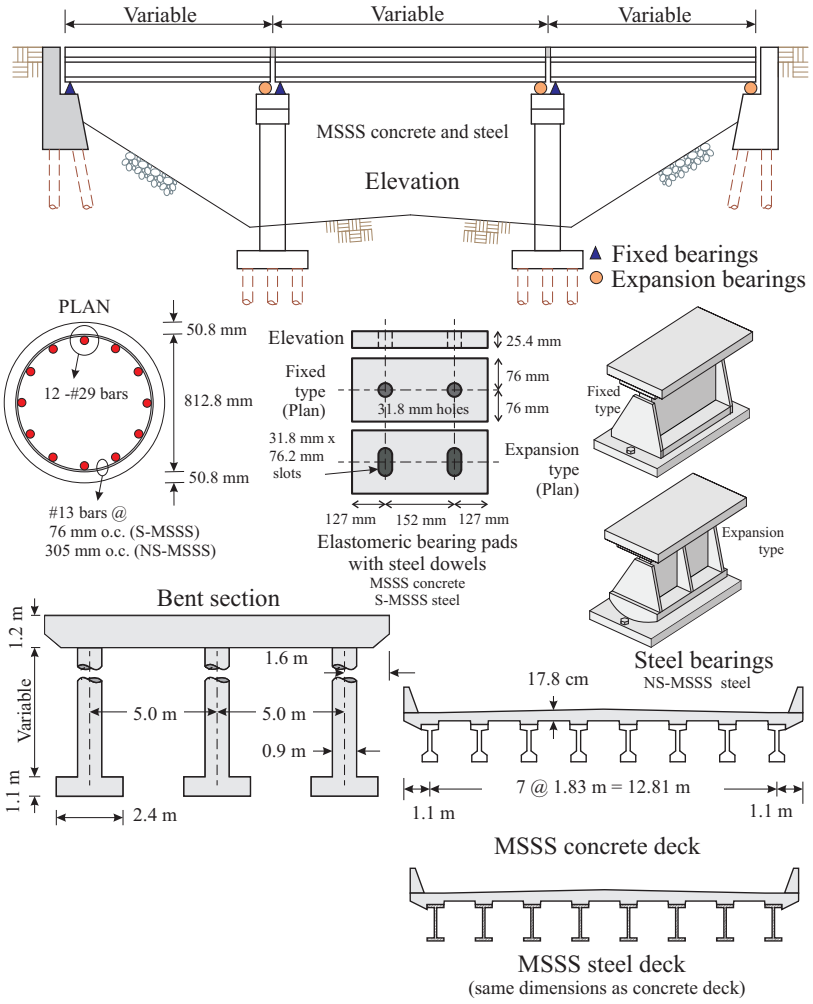

Figure 1: Configuration details of seismically and non-seismically designed bridge classes.

Figure 2 shows various component responses in the MSSS steel girder bridge. Figures 2(a) shows that the column demand is substantially greater in non-seismically designed bridge when compared to its seismic counterpart. In the transverse direction, the seismically designed column experiences a slightly higher moment demand but by far the non-seismically designed column has a much higher curvature demand. The reduced demand on the columns in the seismically designed bridge is due to the increased demand on the bearings. As seen in Figures 2(b) and 2(c), the elastomeric bearing pads in the seismically designed bridge experiences a large force and displacement demand when compared to the brittle steel bearings in the non-seismically designed bridge. The elastomeric bearings have a well defined hysteresis as seen in the figures thereby causing much of the seismic energy to dissipate through enhanced displacement capabilities. It must be noted that in case of steel bearings the internal hysteresis loop captures the frictional component of its response and this frictional force is a function of the normal force that it experiences. In this bridge type, the fixed bearings are typically located at the abutments and the end span, in this case is shorter than the middle span, thereby having a smaller mass and producing smaller reactions leading to narrow hysteresis

loops as depicted in Figure 2(b). This leads to difference in the demand models for these components, as will be shown subsequently in this section. In this case, the abutment response in longitudinal direction is seen to be dominated by passive action as shown in Figure 2(d). The transverse response is characterized by piles alone and in this case, although not shown here, it is seen that the pile action of the abutments never exceeded the linear range with maximum deformations less than 6 mm in either case of seismic and non-seismically designed bridges. Greater pounding action was seen in the non-seismically designed bridge when compared to the seismically designed bridge. Pounding typically causes the passive action of abutments to engage while doing very little to engage the active action. This is depicted in Figure 2(d) where the non-seismically designed bridge has a very dominant passive response (negative quadrant) when compared to the seismically designed bridge. Further, the seismically designed bridge shows very little active response (positive quadrant) which is absent in the case of the non-seismically designed bridge. The transverse load path does not interfere much with pounding and hence very little force gets transmitted to the abutments thereby resulting in the linear response of the abutment piles as seen in this case.

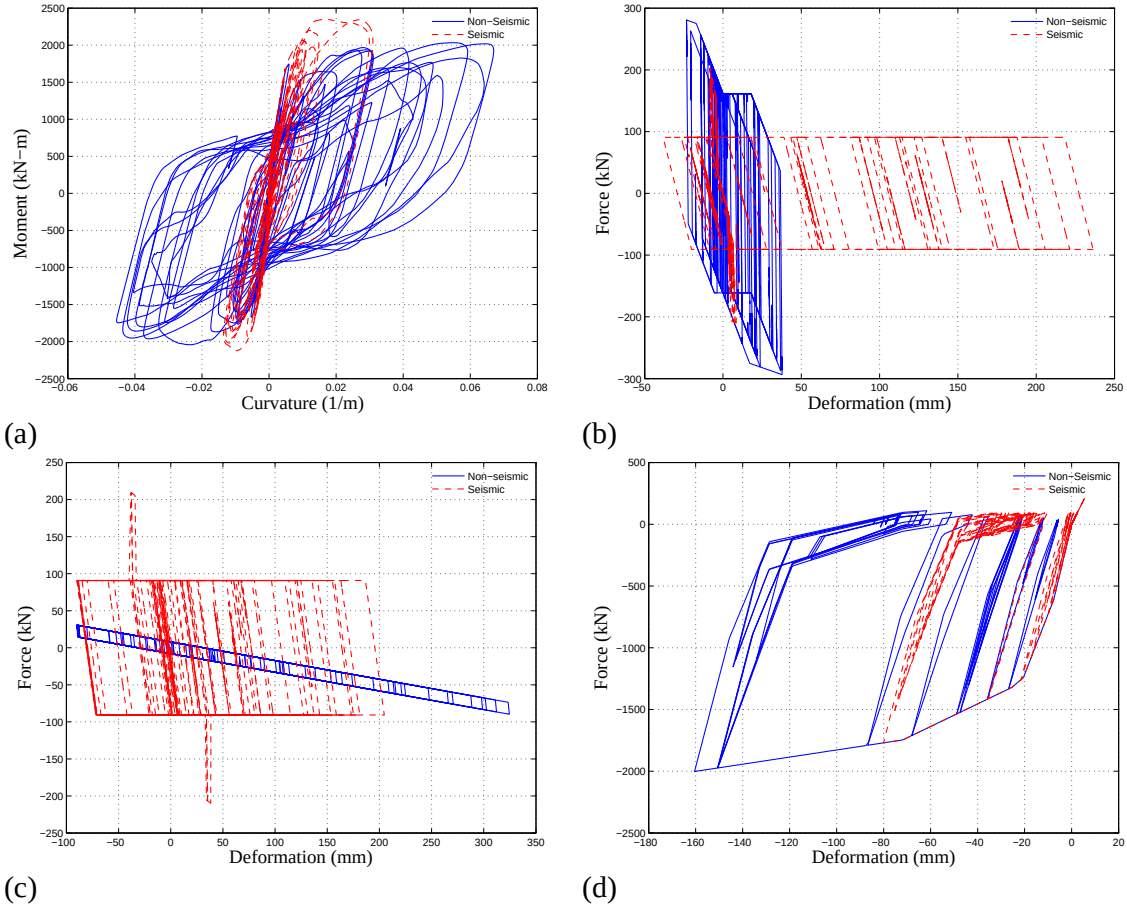

Figure 2: MSSS steel girder bridge component responses for (a) transverse column response, (b) transverse fixed bearing response, (c) longitudinal expansion bearing response, and, (d) longitudinal abutment response.

The component responses from seismically and non-seismically designed MSSS concrete girder bridges with identical geometries and median parameters is shown in Figure 3. As seen in almost all figures 3(a) through 3(d), there is no major difference in demand in the seismically and non-seismically designed bridge. Seismically designed column is seen to have a

slightly greater demand in the transverse direction although both the columns have almost similar demands in the longitudinal direction. The elastomeric bearing pads in the seismically designed bridge were observed to have slightly larger displacement demands when compared to their presence in the non-seismically designed bridge maintain the same force demands. Passive action dominated the abutment response in the longitudinal direction as in the case of steel girder bridges, with the abutments in the seismically designed bridge experiencing slightly greater demands when compared to non-seismically designed bridge. The abutment piles were seen to respond in the elastic range in both the bridges considered similar to steel girder bridges. Therefore, it can be concluded that in case of concrete girder bridge class, the seismic design does not lead to a significant change in the demands and this is reflected in the PSDMs developed subsequently in this section. Instead the change in capacity due to seismic detailing of components is more critical for the concrete bridges.

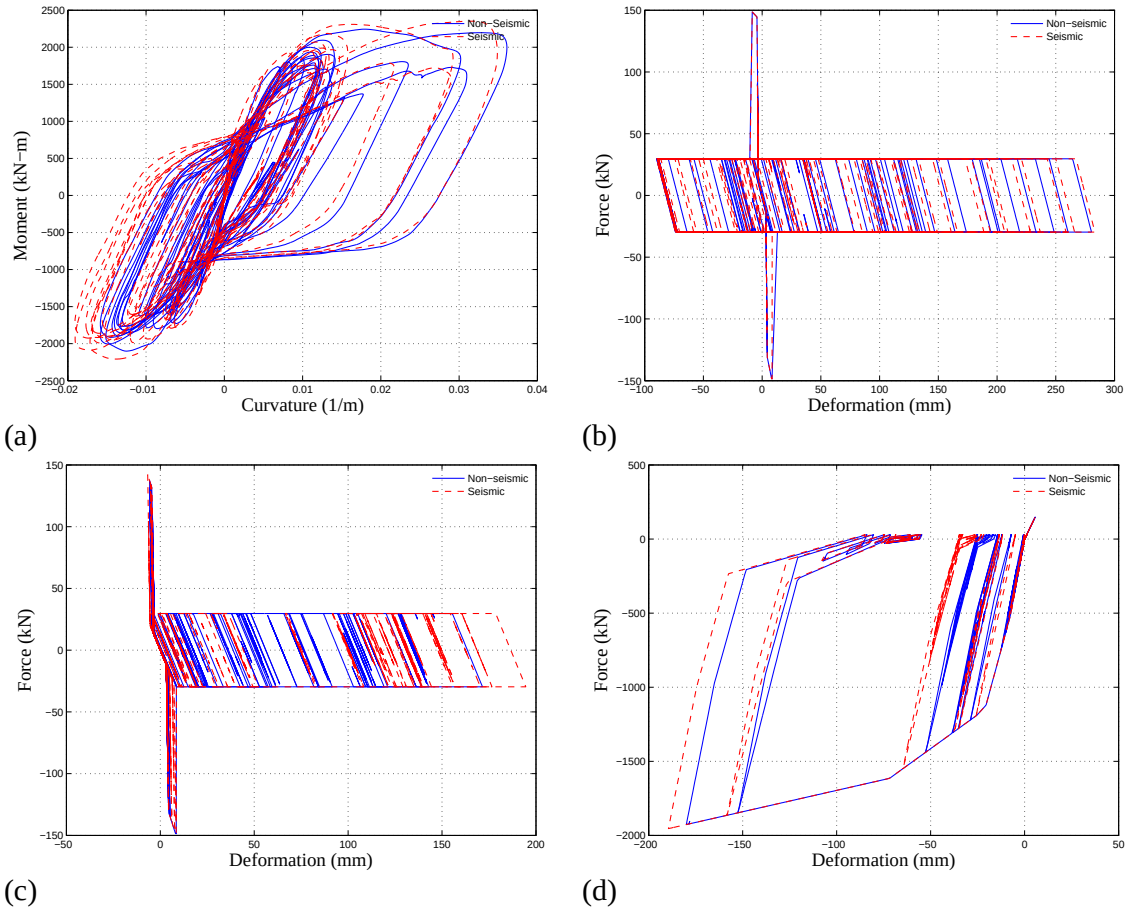

Figure 3: MSSS concrete girder bridge component responses for (a) transverse column response, (b) longitudinal fixed bearing response, (c) transverse expansion bearing response, and, (d) longitudinal abutment response.

3.4 Ground Motion Suite

240 ground motions developed by Fernandez and Rix [29] are used to perform NLTHA. These are probabilistic ground motions developed for selected cities within the Upper Mississippi Embayment including Memphis, TN; Jonesboro, AR; Jackson, TN; Blytheville, AR; Paducah, KY; Cape Girardeau, MO, and Little Rock, AR. Ground motions developed for

Memphis, TN included both Lowlands and Uplands soil profiles since portions of the city are in each soil type. The CSUS ground motions in this database were generated by scaling recorded ground motions for Western United States (WUS). Thus this process provides CSUS ground motions with realistic phase, amplitude relationships between components and frequency-to-frequency variability [29]. The ground motions are probabilistic motions consistent with hazard levels of 10%, 5% and 2% probability of exceedance in 50 years, corresponding to return periods of 475, 975 and 2475 years. 10 motions for each intensity level were generated for every city making it 240 in total. The suite of ground motions is intended to represent the epistemic and aleatoric variability characterized in the soil attenuation relationships developed for the region. Each of the synthetic ground motion was used to generate two orthogonal components following the procedure outlined by Baker and Cornell [30]. The geometric mean of the PGA values of the orthogonal components varies between 0.08g and 1.46g.

3.5 Probabilistic Seismic Demand Models (PSDM)

A PSDM is a conditional statement of the probability that a component experiences a demand for a given IM level, illustrating the importance of the IM as a conditional parameter in the probabilistic model. Hence, the choice of ground motions, definition of the class of structures, formulation of a nonlinear analysis model, and choice of IM and demand measure (DM) pairs form the key aspects of the approach. Padgett et al. [31] and Shafieezadeh et al. [32] explored IMs for portfolios of bridges with geometric variation and concluded that PGA is an optimal IM for probabilistic seismic demand analysis of classes of bridges. This study uses PGA as the IM to develop PSDMs and fragility curves subsequently. The estimation of the median demand, expressed in Equation (1) is based on a power-law model proposed by Cornell et al. [33].

$$S_D = a(IM)^b \tag{1}$$

where, S_D is the median demand, *IM* is the intensity measure chosen, *a* and *b* are the power-law model parameters. By expressing the median demand in logarithmic space, the variation of S_D with the *IM* takes a linear form and this facilitates the evaluation of the parameters *a* and *b* using a simple linear regression analysis. In order to describe the uncertainty about the demand, the logarithmic standard deviation, commonly referred to as the dispersion, $\beta_{D|IM}$, needs to be evaluated, which is expressed in Equation (2). Having estimated, S_D and $\beta_{D|IM}$, the PSDM can be formulated as shown in Equation (3):

$$\beta_{D/IM} = \sqrt{\frac{\sum_{i=1}^{N}\left(\ln d_i - \ln a(IM)^b\right)^2}{N-2}} \tag{2}$$

$$P[D \geq d \mid IM] = 1 - \Phi\left(\frac{\ln(d) - \ln(S_D)}{\beta_{D|IM}}\right) \tag{3}$$

where, $\Phi(\bullet)$ is the standard normal cumulative density function and S_D is shown in Equation (1).

This study considers various geometric and material variabilities in the fragility analysis. As stated previously, twelve representative bridge realizations are created by sampling on the geometric variables obtained from the inventory analyses. In addition to these geometric variations, several other uncertainties are propagated as listed in Table 1. The bridge realizations together with the uncertainties presented in Table 1 are used to create 240 bridge models

which are then randomly paired with 240 Rix ground motions to create 240 bridge – ground motion pairs which are statistically significant and nominally identical.

Uncertainty parameter	Units	Sampling distribution	Distribution parameters	
Concrete compressive strength	MPa	Normal*	$\mu = 33.5$	$\sigma = 4.3$
Reinforcing steel yield strength	MPa	Lognormal†	$\lambda = 6.14$	$\zeta = 0.03$
Elastomeric bearing shear modulus	MPa	Uniform‡	$\alpha = 0.69$	$\beta = 2.07$
Elastomeric bearing coeff. of friction		Lognormal	$\lambda = 0$	$\zeta = 0.1$
Dowel bar strength	MPa	Lognormal	$\lambda = 4.49$	$\zeta = 0.03$
Gap at the dowels	mm	Uniform	$\alpha = 0$	$\beta = 50.8$
Steel fixed bearing coeff. of friction				
Longitudinal direction		Lognormal	$\lambda = -1.56$	$\zeta = 0.5$
Transverse direction		Lognormal	$\lambda = -0.99$	$\zeta = 0.5$
Steel expansion bearing coeff. of friction				
Longitudinal direction		Lognormal	$\lambda = -3.22$	$\zeta = 0.5$
Transverse direction		Lognormal	$\lambda = -2.30$	$\zeta = 0.5$
Passive abutment stiffness	kN/mm/m	Uniform	$\alpha = 11.5$	$\beta = 28.8$
Active abutment stiffness	kN/mm/m	Uniform	$\alpha = 2.2$	$\beta = 6.6$
Translational foundation stiffness	kN/mm/pile	Uniform	$\alpha = 28$	$\beta = 84$
Rotational foundation stiffness	kN-m/rad	Uniform	$\alpha = 3\ (10)^5$	$\beta = 9.1(10)^5$
Deck mass ratio		Uniform	$\alpha = 0.9$	$\beta = 1.1$
Damping ratio		Normal	$\mu = 0.045$	$\sigma = 0.0125$
Gap at internal hinges	mm	Normal	$\mu = 25.4$	$\sigma = 4.3$
Gap between deck and abutment	mm	Normal	$\mu = 38.1$	$\sigma = 5.8$
Earthquake angle of incidence	rad	Uniform	$\alpha = 0$	$\beta = 2\pi$

*Normal distribution is characterized by the mean, μ, and standard deviation, σ.
†Lognormal distribution is characterized by the parameters, λ and ζ, which are the mean and standard deviation, respectively, of the associated normal distribution.
‡Uniform distribution is characterized by the lower, α, and upper bound, β.

Table 1: List of uncertainties considered in fragility analysis.

A full NLTHA is performed for each bridge – ground motion pair and the maximum demand placed on various components is recorded. In total, 1920 NLTHA are performed for the seismically and non-seismically designed bridges in the four bridge classes considered. Researches in the past [16, 17, 18] have indicated the necessity to consider the vulnerability of several key components to assess system level performance and hence this study considers multi-component vulnerability. Table 2 details the demand parameters used to assess component demands for various bridge components considered in this study. Having performed NLTHA and recorded peak component demands, PSDMs are determined according to the procedure described in the previous section, according to the formulations in Equations (1), (2) and (3).

Demand measure	Abbreviation	Units
Column curvature ductility demand	μ_ϕ	
Longitudinal fixed bearing deformation	δ_{fl}	mm
Transverse fixed bearing deformation	δ_{ft}	mm
Longitudinal expansion bearing deformation	δ_{el}	mm
Transverse expansion bearing deformation	δ_{et}	mm
Passive abutment deformation	δ_p	mm
Active abutment deformation	δ_a	mm

Transverse abutment deformation	δ_t	mm

Table 2: Bridge component demand measures.

Figure 4 illustrates a few sample PSDMs for S-MSSS and NS-MSSS concrete and steel girder bridge classes for the columns and bearings. There is a very minor difference in demand in S-MSSS and NS-MSSS concrete bridges as seen in Figures 4(a) and 4(b). This is expected since the initial stiffness for both cases is identical, and the maximum compressive strength only shows in small difference between the seismically and non-seismically designed bridge columns. The critical effect of the non-seismically designed column is not necessarily an effect on the demand but rather a reduction in capacity. Hence, limit states are most critical when considering changes only in column detailing. However, in the case of the steel bridges, an appreciable difference in demand curves is observed as shown in Figures 4(c) and 4(d) for MSSS steel girder bridges. The difference in the dynamic characteristics of the bridge and the change in load path, as explained in the early parts of this section, are the predominant reasons for the difference in demand models.

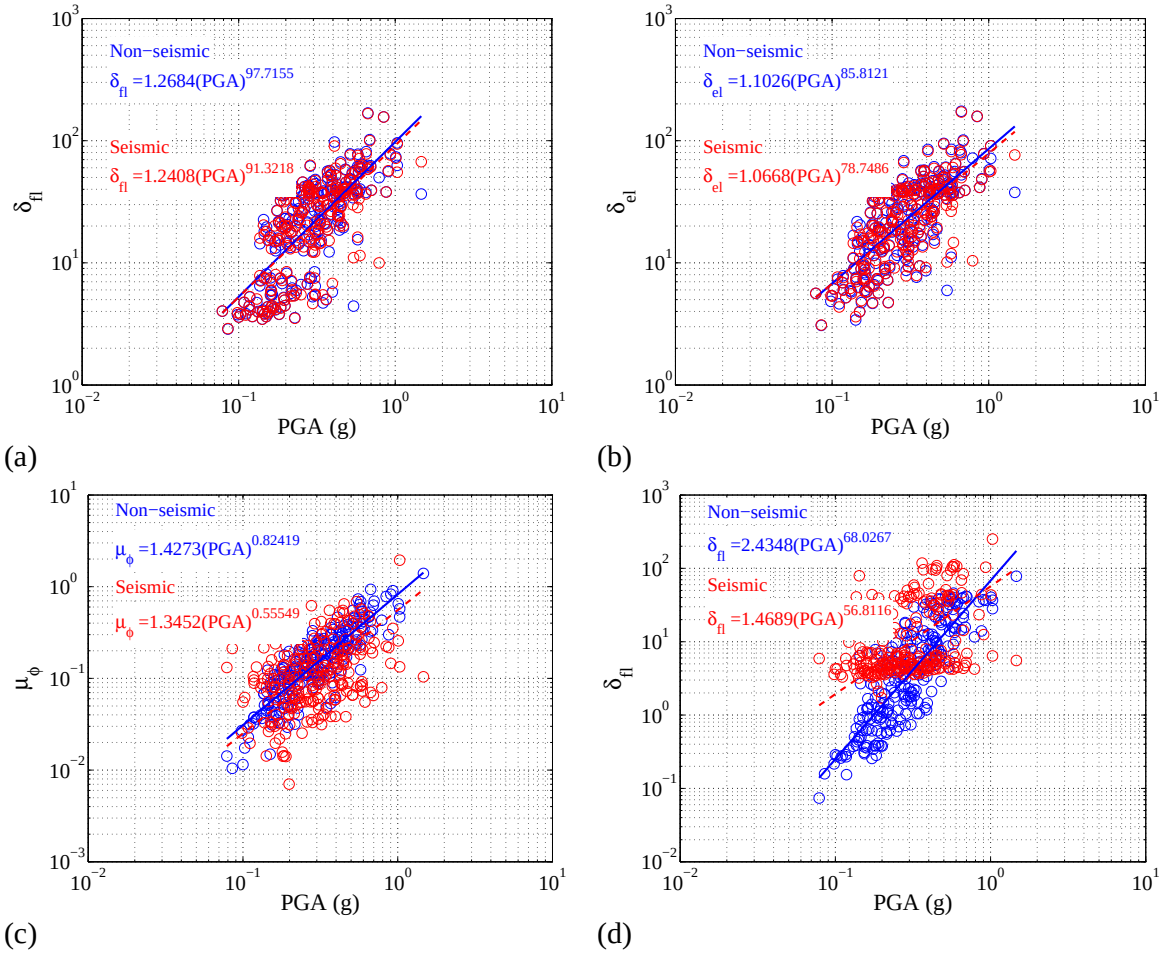

Figure 4: Probabilistic seismic demand models for (a) longitudinal fixed bearing response in MSSS concrete, (b) longitudinal expansion bearing response in MSSS concrete, (c) columns in MSSS steel, and (d) longitudinal fixed bearing response in MSSS steel.

3.6 Component Damage States

The components considered in this study are columns, fixed and expansion elastomeric bearings and abutments (active and passive as well as transverse).The component limit states are also assumed to be lognormally distributed. The median, S_c and the dispersion, β_c values of the capacity limit states are obtained from experimental results and are truly prescriptive. The study uses four damage states; slight, moderate, extensive and complete, comparable to those found in HAZUS-MH. Table 3 summarizes the limit states adopted for the various bridge components. The damage state definitions provided in Table 3 stem from recommendations from previous studies [12, 21, 16, 18] and results from experimental tests. The damage states for columns are quantified using curvature ductility and the results presented in the table below for seismically and non-seismically designed columns stem from the recommendations of [12] and the Pacific Earthquake Engineering Research (PEER) Center's column structural performance database [34]. Steel fixed and expansion bearings have damage states prescribed in terms of displacements and the values shown in Table 3 are obtained from experimental tests conducted on similar bearings [26]. The bearing damage states for elastomeric bearing pads and those for the abutments are consistent with those presented in [16].

Component	Slight		Moderate		Extensive		Complete	
	S_c	β_c	S_c	β_c	S_c	β_c	S_c	β_c
Columns								
Non-seismically designed	1.0	0.25	1.58	0.25	3.22	0.47	4.18	0.47
Seismically designed	1.0	0.25	5.11	0.25	7.50	0.47	9.00	0.47
Elastomeric bearing pads with steel dowels								
Fixed bearing – Long. (mm)	30.0	0.25	100.0	0.25	150.0	0.47	255.0	0.47
Fixed bearing – Trans. (mm)	30.0	0.25	100.0	0.25	150.0	0.47	255.0	0.47
Expansion bearing – Long. (mm)	30.0	0.25	100.0	0.25	150.0	0.47	255.0	0.47
Expansion bearing – Trans (mm)	30.0	0.25	100.0	0.25	150.0	0.47	255.0	0.47
Steel bearings								
Fixed bearing – Long. (mm)	6.0	0.25	20.0	0.25	40.0	0.47	255.0	0.47
Fixed bearing – Trans. (mm)	6.0	0.25	20.0	0.25	40.0	0.47	255.0	0.47
Expansion bearing – Long. (mm)	6.0	0.25	20.0	0.25	40.0	0.47	255.0	0.47
Expansion bearing – Trans (mm)	30.0	0.25	100.0	0.25	150.0	0.47	255.0	0.47
Abutments								
Passive response (mm)	37.0	0.25	146.0	0.25	1000	0.47	1000	0.47
Active response (mm)	9.75	0.25	37.9	0.25	77.2	0.47	1000	0.47
Transverse response (mm)	9.75	0.25	37.9	0.25	77.2	0.47	1000	0.47

Table 3: Prescriptive bridge component limit states.

3.7 Component Fragility Curves

Fragility curves at the component level are derived based on the formulation presented in Equation (4) to provide a basis of comparison for the effect of seismic detailing on component vulnerability for the various bridge classes.

$$P[D > C \mid IM] = \Phi\left(\frac{\ln(S_D/S_c)}{\sqrt{\beta_{D|IM}^{\ 2} + \beta_c^{\ 2}}}\right) \tag{4}$$

Figure 5 plots the component fragilities for the S-MSSS concrete and steel girder bridges at the two intermediate limit states. In the case of the S-MSSS steel bridge class, the elasto-

meric expansion bearings are the most vulnerable component at the slight damage state whereas the elastomeric fixed bearings tend to be the most vulnerable component at all the other damage states as shown in Figures 5(a) and 5(b). This should be expected as there was considerable demand imposed on the bearings as illustrated in Section 3.5 and Figure 2. In the case of NS-MSSS steel, the columns tend to be the most vulnerable component at lower damage states while the longitudinal expansion bearing response dominates the system fragility at higher damage states. This shift in vulnerability may be attributed to the change in dynamic characteristics and resulting demands imposed on the components due to the consideration of seismic design principles. In the case of the S-MSSS concrete bridge class, as shown in Figures 5(c) and 5(d), the expansion bearings tend to dominate the vulnerability in the slight and moderate damage states but the fixed bearings dominate the vulnerability in the case of the extensive and complete damage states. In contrast, columns tend to dominate the vulnerability of the system at all damage states.

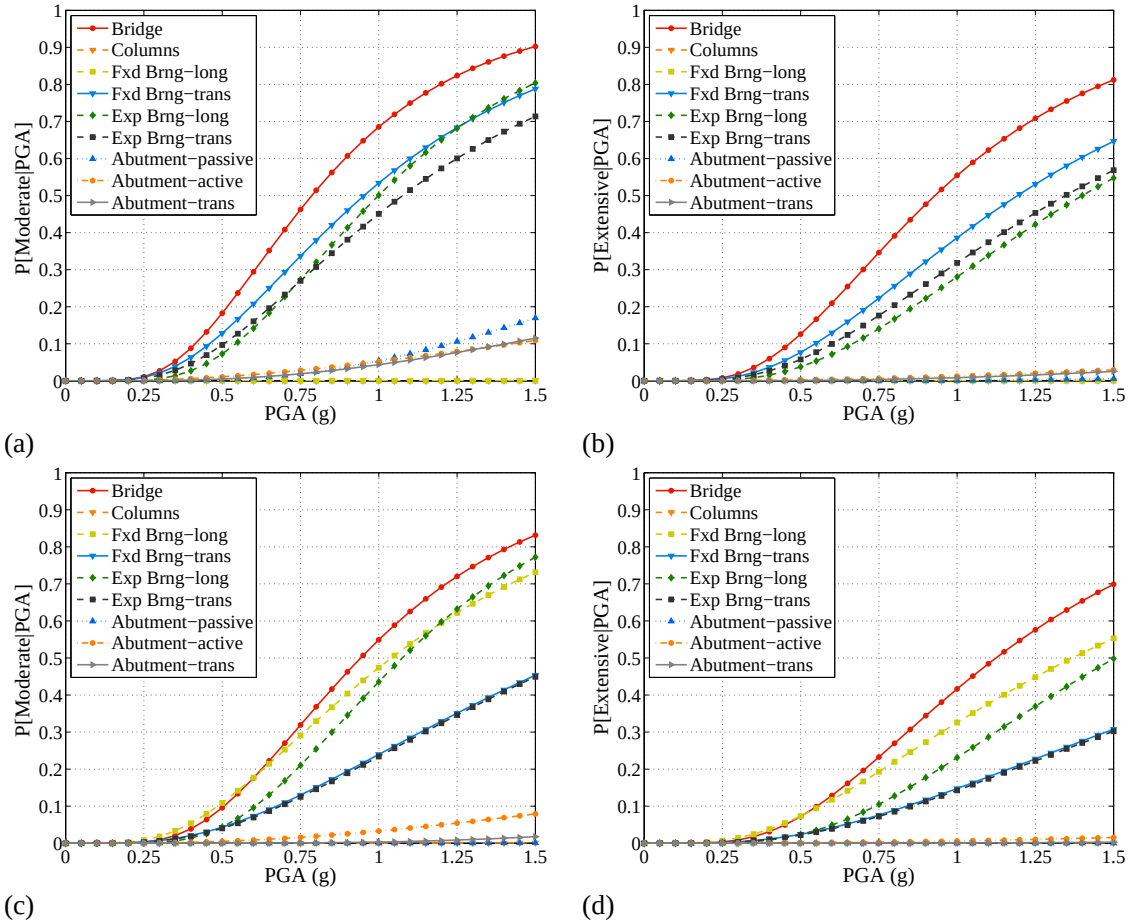

Figure 5: Bridge and component fragility curves for S-MSSS steel girder bridge class for (a) moderate, and (b) extensive limit states, and for S-MSSS concrete girder bridge class for (c) moderate, and (d) extensive damage states.

4 BRIDGE SYSTEM FRAGILITY CURVES

4.1 Comparison of System Fragility for Seismically and Non-seismically Designed Bridge Classes

The logical step that succeeds the determination of component fragilities is to integrate these to enable the macroscopic view of the bridge as a system. Several researchers [16, 35, 21] have proposed techniques to develop fragility curves for the bridge as a system. Mackie and Stojadinovic [35] used the first order reliability method in developing fragility curves while Choi et al. [21] considered first order bounds for series systems. The present study uses the approach developed by [16]. The estimate of system fragility curves is facilitated through the development of joint probabilistic seismic demand model (JPSDM), recognizing that the demands on various components have some level of correlation. A Monte Carlo simulation is then used to compare realizations of the demand (using the JPSDM defined by a conditional joint normal distribution in the transformed space) and statistically independent component capacities to calculate the probability of system failure. Samples (10^6 in this case) are drawn from both the demand and capacity models and the probability of demand exceeding the capacity is evaluated for a particular IM value. The procedure is repeated for increasing values of the IM. Regression analysis is used to estimate the lognormal parameters, median and dispersion, which characterize the bridge system fragility. The methodology presented in this section is used to develop system fragility curves for seismically and non-seismically designed bridges within the fore mentioned bridge classes by considering multiple component vulnerability. The CDFs that define the probabilities of exceeding a limit state, LS, can then be plotted based on the Equation (5), where λ_i and ζ_i are the median and dispersion, respectively, of the i^{th} limit state.

$$P[LS \mid IM] = \Phi\left(\frac{\ln(IM) - \ln(\lambda_i)}{\zeta_i}\right) \tag{5}$$

Figure 6 shows the system fragility curves for seismic and non-seismically designed MSSS concrete and steel girder bridge classes. In the case of the MSSS concrete bridge class, a very minor difference is seen in the curves at slight damage state. This is because the elastomeric expansion bearings dominate the vulnerability at this limit state followed by elastomeric fixed bearings. Hence, a significant improvement is not seen due to seismic detailing of the columns which has little effect on the demand and more effect on the capacity. On the contrary, in case of the MSSS steel bridge class, significant differences are observed in the curves at all damage states as shown in Figure 6(b). These differences may be attributed predominantly to the replacement of the non-ductile steel bearings with elastomeric bearing pads. This is not the case in their concrete bridge counterparts as the only difference between seismic and non-seismic design is with respect to the column ductility enhancement. Steel bearings are the most vulnerable components in case of NS-MSSS steel bridge class and hence their replacement along with seismic detailing of columns produces a significant reduction in the vulnerability of the system as a whole. This is seen in Figure 6(b).

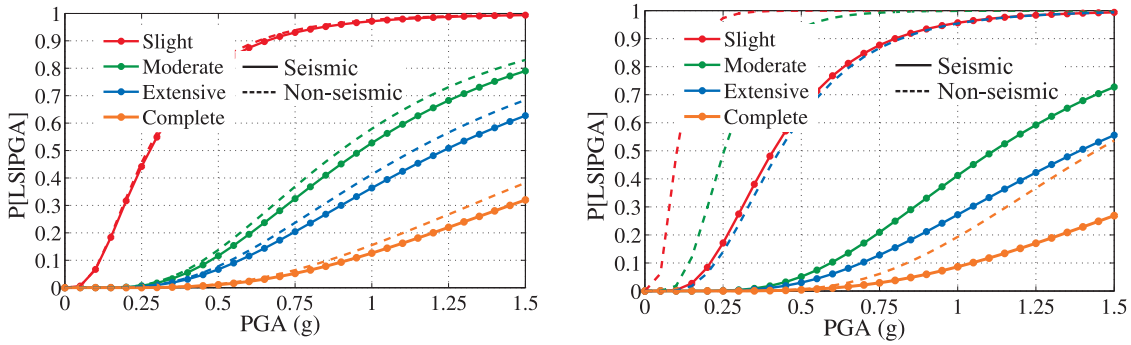

Figure 6: Bridge system fragility curves for seismically and non-seismically designed (a) MSSS concrete girder bridge class, and (b) MSSS steel girder bridge class.

In the case of all the bridge classes, with and without seismic design, the dispersions associated with various limit states fall in a narrow range and hence a single constant dispersion value is chosen to characterize the bridge fragility curves. For example, in the case of the S-MSSS concrete girder bridge class, the dispersion values for slight, moderate, extensive and complete damage states are 0.50, 0.56, 0.52, and 0.55 respectively. In this case, a constant dispersion equal to the mean value, 0.53 in this case, is chosen for the curves corresponding to all the limit states. The median values of fragility curves for the bridge system for various bridge classes along with the dispersions is tabulated in Table 4. It can be seen that incorporation of seismic design principles tends to increase the dispersion about the median fragility. In this study, the parameters included in the uncertainty analysis are the same for both seismic and non-seismically designed bridges, and these were obtained from a sensitivity study presented in [16] that was primarily aimed as non-seismically designed bridge classes. The dispersions associated with the various damage states are similar for seismically and non-seismically designed bridge classes.

Bridge class	Seismically designed*					Non-seismically designed					Percent change in λ			
	λ_s†	λ_m	λ_e	λ_c	ζ	λ_s	λ_m	λ_e	λ_c	ζ	λ_s	λ_m	λ_e	λ_c
MSSS concrete	0.37	0.94	1.12	1.66	0.53	0.34	0.84	0.99	1.41	0.46	8.8	11.9	13.1	17.7
MSSS steel	0.41	1.12	1.39	2.09	0.52	0.10	0.26	0.43	1.45	0.46	310	331	223	44.1

*The subscripts s, m, e, c for the median values denote slight, moderate, extensive and complete damage states, respectively.
†Median values are reported as proportions of acceleration due to gravity, *g*.

Table 4: Median and dispersion values for bridge class fragility and percentage change in median values of between seismically and non-seismically designed bridge classes.

A simple technique to compare differences in the fragility curves is to evaluate the relative change in the median value of the fragility curves. This facilitates comparison between the bridge classes as well as for seismic and non-seismic detailing of a given bridge type. A positive change indicates a less vulnerable structure while a negative change indicates a more vulnerable structure. The percentage change in median values for the seismically designed bridges with respect to their non-seismic counterparts is also reported in Table 4. As mentioned previously, significant improvements in the median values are seen in case of the steel bridges in comparison to the marginal improvements in case of concrete bridges. The higher percentage increase in case of steel bridges can be attributed to the seismic detailing provisions in the columns and replacement of the steel bearings with the elastomeric bearing pads.

The results show that the difference in the median values is well pronounced at higher damage states when compared to lower states. This can be attributed to the fact that the actual distinction in performance is predominant when significant nonlinearity occurs and this is seen typically at higher damage states. Hence, the effect of seismic design is well pronounced at the higher damage states.

4.2 Comparisons with HAZUS

As mentioned in Section 1 of the paper, the fragility curves currently used in the risk assessment software, HAZUS, were developed by Basoz and Mander [14] using the nonlinear static procedure, commonly referred to as the Capacity Spectrum Method. These fragility curves, akin to the ones developed in this study are applicable to a class of bridges. The dispersions for the system fragility curves obtained in this study are in the range of 0.5-0.6 (see Table 4) and this is in good agreement with the value of 0.6 proposed by Basoz and Mander [14]. Table 5 shows the median value of fragilities obtained from this study along with the values used in HAZUS-MH. The percentage change in the median values of the present study with respect to those in HAZUS-MH is also presented. A positive change in the median values indicates a less vulnerable structure while a negative change indicates a more vulnerable structure.

Bridge class	Source	Median (g) values				Percentage change (%)			
		λ_s	λ_m	λ_e	λ_c	λ_s	λ_m	λ_e	λ_c
S-MSSS concrete	Proposed	0.37	0.94	1.12	1.66	-17.8	23.7	6.7	8.50
	HAZUS	0.45	0.76	1.05	1.53				
NS-MSSS concrete	Proposed	0.34	0.84	0.99	1.41	30.8	14.0	25.0	16.9
	HAZUS	0.26	0.35	0.44	0.65				
S-MSSS steel	Proposed	0.41	1.12	1.39	2.09	-8. 9	47.4	32.4	36.6
	HAZUS	0.45	0.76	1.05	1.53				
NS-MSSS steel	Proposed	0.1	0.26	0.43	1.45	-61.5	-25.7	-2.3	23.1
	HAZUS	0.26	0.35	0.44	0.65				

Table 5: Median values of fragility curves obtained in this study and those from HAZUS.

For the seismically and non-seismically designed bridge classes, this study shows that the bridges are much less vulnerable in the complete damage state. The difference in median values proposed in this study to those reported in HAZUS-MH could be attributed to a variety of reasons. This study adopts nonlinear time history analyses while the fragilities reported in HAZUS-MH are derived using nonlinear static procedure. The differences are also attributed to the consideration of multiple components in estimating the overall system vulnerability and differences in the limit state values. Further, this study considers a much broader list of geometric and material variables in the fragility framework in addition to inclusion of key bridge class attributes based on a detailed NBI bridge inventory. The hallmark of this study is that it also includes considerations of seismic, non-seismic, and general design features exclusive to bridge classes predominant in CSUS making these fragility estimates more suitable to this region.

5 CONCLUSIONS

This study presents an analytical method for the development of fragility curves for seismically and non-seismically designed bridge classes in the central and southeastern United States. Two typical multispan bridge classes are considered that include simply supported

concrete and steel girder bridges. Detailed three dimensional finite element models which account for the nonlinear behavior of the column, girders, and abutments, are developed in the OpenSEES platform. Fragility curves are developed from nonlinear time history analyses using a suite of 240 ground motions developed by Fernandez and Rix [29] for selected cities within the Upper Mississippi Embayment. The uncertainty analysis includes a range of material and geometric parameters and the fragility curves are developed considering multiple component vulnerability using the joint probabilistic seismic demand model approach developed by Nielson and DesRoches [16]. The predominant difference between seismically and non-seismically designed bridges is associated with enhanced ductility characteristics of the column in all the bridge classes considered. In the case of steel girder bridge class, the non-ductile steel bearings prevalent in non-seismically designed bridges are replaced with elastomeric bearing pads with steel dowels in bridges designed post 1990.

The following are some of the important conclusions that can be drawn from the present study. Significant reduction in the vulnerability is seen in both the bridge classes considered in this study with seismic design principles used in their design. The percentage change in the median values is as high as 300% for almost all damage states in the case of steel girder bridges and it is to the order of 15% in the case of their concrete counterparts. The big increase in steel bridges may be attributed to enhanced column ductility performance and replacement of non-ductile steel bearings with elastomeric bearing pads. Comparisons are made between the proposed fragility curves and with those presently adopted by HAZUS-MH. For the seismically and non-seismically designed bridge classes, this study yields significantly fewer vulnerable bridge classes at the complete damage state. The results from this study yield significantly less vulnerable seismically designed bridge fragilities in comparison to HAZUS-MH. The differences in median fragilities may be attributed to the difference in the adoption of analyses techniques, definition of system vulnerability, range of parameters considered in the stochastic analysis at the least. This study considers seismic, non-seismic, and general design features exclusive to bridge classes predominant in CSUS making these fragility estimates more suitable to this region.

REFERENCES

[1] R. V. Whitman, J. M. Biggs, J. E. Brennan III, A. C. Cornell, R. L. de Neufville, and E. H. Vanmarcke, Seismic Design Decision Analysis. *Journal of Structural Engineering*, 101, 1067-1084, 1975.

[2] ATC, 1985. Earthquake Damage Evaluation Data for California, *Report No. ATC – 13*, Applied Technology Council, Redwood City, CA.

[3] ATC, 1991. Seismic Vulnerability and Impact of Disruption of Lifelines in the Coterminous United States, *Report No. ATC – 25*, Applied Technology Council, Redwood City, CA.

[4] FEMA, 2003. *HAZUS-MH MR1: Technical Manual.* Federal Emergency Management Agency, Washington, DC.

[5] Basoz, N., and Kiremidjian, A. S., 1997. Evaluation of Bridge Damage Data from the Loma Prieta and Northridge CA Earthquakes, *Report No. MCEER-98-0004*, MCEER, Buffalo, NY.

[6] Yamazaki, F., Hamada, T., Motoyama, H., and Yamauchi, H., 1999. Earthquake Damage Assessment of Expressway Bridges in Japan, *Technical Council on Lifeline Earthquake Engineering Monograph*, 16, 361-370.

[7] Der Kiureghian, A., 2002. Bayesian Methods for Seismic Fragility Assessment of Lifeline Components, *Acceptable Risk Processes: Lifelines and Natural Hazards*, Monograph No. 21, A. D. Kiureghian ed., Technical Council for Lifeline Earthquake Engineering, ASCE, Reston, VA.

[8] Shinozuka, M., Feng, M. Q., Kim, H.-K., and Kim, S.-H., 2000. Nonlinear Static Procedure for Fragility Curve Development, *Journal of Engineering Mechanics*, **126(12)**, 1287-1296.

[9] Shinozuka, M., Feng, M. Q., Kim, H., Uzawa, T. and Ueda, T., 2003. Statistical Analysis of Fragility Curves, *Report No. MCEER-03-0002*, MCEER, Buffalo, NY.

[10] Elnashai, A., Borzi, B., and Vlachos, S., 2004. Deformation-Based Vulnerability Functions for RC Bridges, *Structural Engineering and Mechanics*, **17(2)**, 215-244.

[11] Yu. O., Allen, D. L., and Drnevich, V. P., 1991. Seismic Vulnerability Assessment of Bridges on Earthquake Priority Routes in Western Kentucky, *3rd US National Conference on Lifeline Earthquake Engineering*, Los Angeles, CA.

[12] Hwang, H., Jernigan, J. B., and Lin, Y. W., 2000. Evaluation of seismic damage to Memphis bridges and highway systems, *Journal of Bridge Engineering* **5(4)**, 322-330.

[13] Dutta, A., 1999. On Energy Based Seismic Analysis and Design of Highway Bridges, *Ph.D. Thesis*, State University of New York at Buffalo, Buffalo, NY.

[14] Basoz, N., and Mander, J. B., 1999. *Enhancement of the Lifeline Transportation Module in HAZUS, Report No. Draft #7*, National Institute of Building Sciences, Washington, DC.

[15] Mackie, K., and Stojadinovic, B., 2005. Fragility Basis for California Highway Overpass Bridge Seismic Decision Making, *PEER Report 2005/02*, Pacific Earthquake Engineering Research Center, University of California, Berkeley, CA.

[16] Nielson, B. G., and DesRoches, R., 2007. Analytical Seismic Fragility Curves for Typical Bridges in the Central and Southeastern United States, *Earthquake Spectra* **23**, 615-633.

[17] Padgett, J. E., and DesRoches, R., 2008. Methodology for Development of Analytical Fragility Curves for Retrofitted Bridges, *Earthquake Engineering and Structural Dynamics*, **37(8)**, 1157-1174.

[18] Ramanathan, K., DesRoches, R., Padgett, J. E., 2010. Analytical Fragility Curves for Multispan Continuous Steel Girder Bridges in Moderate Seismic Zones, *Transportation Research Record* 2202, 173-182.

[19] U.S. Department of Transportation, Federal Highway Administration, 2009. *National Bridge Inventory Data*, Washington, DC, available at: http://www.fhwa.dot.gov/bridge/nbi/ascii.cfm.

[20] DesRoches, R., Choi, E., Leon, R. T., Dyke, S. J., and Aschheim, M., 2004. Seismic Response of Multiple Span Steel Bridges in Central and Southeastern United States. I: As Built, *Journal of Bridge Engineering* **9(5)**, 464-473.

[21] Choi, E., DesRoches, R., and Nielson, B., 2004. Seismic Fragility of Typical Bridges in Moderate Seismic Zones, *Engineering Structures* **26(2)**, 187–199.

[22] Mander, J. B., Priestley, M. J. N., and Park, R., 1988. Theoretical stress-strain model for confined concrete, *Journal of Structural Engineering* **114(8)**, 1804-1826.

[23] Bignell, J. L., LaFave, J. M., and Hawkins, N. M., 2005. Seismic vulnerability assessment of wall pier supported highway bridges using nonlinear pushover analysis, *Engineering Structures* **27**, 2044-2063.

[24] McKenna F., Scott M., and Fenves G. L., 2010. Nonlinear Finite-Element Analysis Software Architecture Using Object Composition, *Journal of Computing in Civil Engineering* **24(1)**, 95-107.

[25] Muthukumar, S., and DesRoches, R., 2006. A Hertz contact model with non-linear damping for pounding simulation, *Earthquake Engineering and Structural Dynamics* **35**, 811-828.

[26] Mander, J. B., Kim, D. K., Chen, S. S., Premus, G. J., 1996. Response of steel bridge bearings to reversed cyclic loading, *Technical Report NCEER 96-0014*, Buffalo, NY.

[27] Caltrans, 1990. *Caltrans Structures Seismic Design References*, First Edition, California Department of Transportation, Sacramento, CA.

[28] Ma, Y., and Deng, N., 2000. *Deep Foundations, Bridge Engineering Handbook*, Chen, W.-F., and Duan, L. (editor) CRC Press.

[29] Fernandez, J. A., and Rix, G. J., 2006. Probabilistic Ground Motions for Selected Cities in the Upper Mississippi Embayment, available at: http://geosystems.ce.gatech.edu/soil_dynamics/research/groundmotionsembay/.

[30] Baker, J., and Cornell, A. C., 2006. Which Spectral Acceleration Are You Using? *Earthquake Spectra* **22**, 293-312.

[31] Padgett, J. E., Nielson, B. G., and DesRoches, R., 2008. Selection of optimal intensity measures in probabilistic seismic demand models of highway bridge portfolios, *Earthquake Engineering and Structural Dynamics* **37**, 711-725.

[32] Shafieezadeh, A., Ramanathan, K., Padgett, J. E., and DesRoches, R., 2010. Fractional Order Intensity Measures for Probabilistic Seismic Demand Modeling Applied to Highway Bridges, *Earthquake Engineering and Structural Dynamics*, In Press.

[33] Cornell, A. C., Jalayer, F., Hamburger, R. O., and Foutch, D. A., 2002. Probabilistic basis for 2000 SAC Federal Emergency Management Agency steel moment frame guidelines, *Journal of Structural Engineering* **128**, 526-532.

[34] Berry, M. P., and Eberhard, M. O., 2004. *PEER Structural Performance Database User's Manual*, Pacific Earthquake Engineering Research Center, University of California, Berkeley CA.

[35] Mackie, K., and Stojadinovic, B., 2004. Fragility curves for reinforced concrete highway over-pass bridges, *13th World Conference on Earthquake Engineering, August 2004*, Vancouver, B.C., Canada.